On Transfemoral Prosthetic Knee Design Using RRSS Motion and Axode Generation

J. D'Alessio, K. Russell and R.S. Sodhi

Abstract In this work, equation systems for RRSS motion generation and RRSS axode generation are applied to produce a concept transfemoral prosthetic knee. First, an RRSS linkage is synthesized to approximate a series of tibial positions during knee flexion. Next, the fixed and moving axodes of the synthesized RRSS linkage are generated. Because the coupler motion of an RRSS linkage can be replicated by rolling its moving axode over its fixed axode, the axodes for the synthesized RRSS linkage are incorporated as gearing in the concept prosthetic knee. The resulting prosthetic knee approximates the natural spatial motion of the tibia during knee flexion and extension (unlike prosthetic knee designs that include simple pin joints).

Keywords Spatial linkage · RRSS linkage · Motion generation · Axode generation · Transfemoral prosthesis

1 Introduction

Knee motion in the human leg can be described by three rotations and three translations in the principle planes of motion, namely the coronal or frontal plane, the sagittal or side plane and the transverse or horizontal plane (Fig. 1). Natural knee motion initially was characterized by purely planar motion in the sagittal plane [1]. It is now well understood natural knee motion doesn't occur solely in this plane. A complex motion of the principal rotations and translations has been

J. D'Alessio
Onkos Surgical, Parsippany, USA
e-mail: Jdalessio@onkossurgical.com

K. Russell (✉) · R.S. Sodhi
New Jersey Institute of Technology, Newark, USA
e-mail: kevin.russell@njit.edu

R.S. Sodhi
e-mail: rajpal.s.sodhi@njit.edu

J. Beran et al. (eds.), *Advances in Mechanism Design II*,
Mechanisms and Machine Science 44, DOI 10.1007/978-3-319-44087-3_4

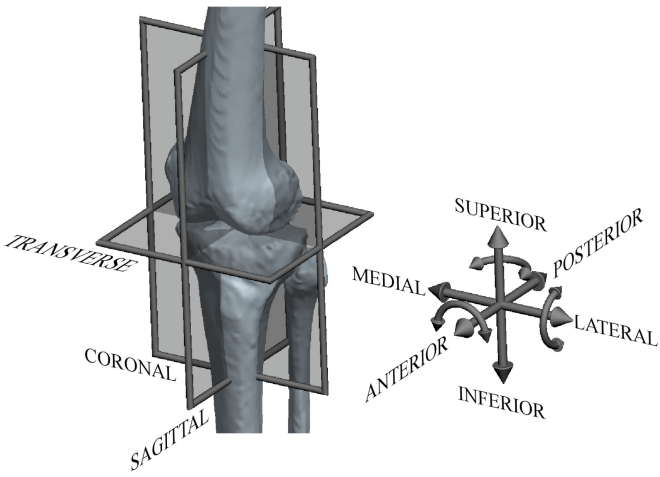

Fig. 1 Planes, rotations and translations for knee motion

documented [2, 3]. Additionally, research has shown that these rotations and translations can be described by showing how the tibia undergoes *screw motion* about the femur [4–7]. The same research has also shown that the position and orientation of this screw axis (called the *finite helical axis*) changes continuously throughout knee motion due to the complex 3D motion occurring in all three planes.

Because knee motion is helical over a continuously-changing axis and does not occur entirely in the sagittal plane, representing the knee as a simple pin or even a polycentric joint (where motion is restricted to pure rotation) in a transfemoral prosthetic leg design results in a prosthesis that does not achieve the natural spatial motion of the tibia. The user of this type of prosthesis will exhibit an unnatural gait to compensate for the unnatural prosthetic knee motion.

2 Design Processes and Models

Figure 2 illustrates the three stages in the prosthetic knee design process and the output from each stage. First, a series of tibial position data are acquired over a determined knee motion range. Next, this data is incorporated in a model to synthesize a spatial *revolute-revolute-spherical-spherical* or RRSS linkage to approximate the tibial positions. After this, the dimensions for the synthesized RRSS linkage are incorporated in a model to generate its fixed and moving axodes over the calculated RRSS motion range. Lastly, the fixed and moving axodes are incorporated into geometry (as gearing) to produce the cam components in the prosthetic knee.

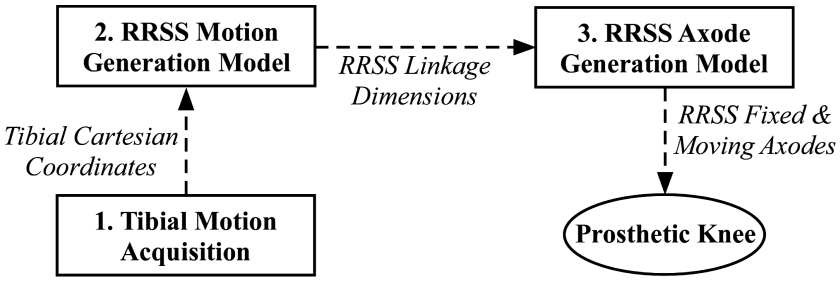

Fig. 2 Stages in transfemoral prosthetic knee design process

Figure 3 illustrates the workstation used in this work to measure tibial-femoral positions. The *localizer* measures and records position coordinates (in spatial Cartesian form) from *trackers*. Trackers are mechanically affixed directly to the tibia and femur bones. A direct tracker-to-bone connection (rather than tracker-to-skin connection), eliminates the bone position error introduced by the motion of leg skin tissue and muscle tissue. In this work, a cadaveric leg specimen was utilized. Not shown in Fig. 3 is the system of pulleys and cables used to support and actuate the cadaver leg from full flexion to full extension.

Russell and Shen [8] presented a motion generation model to synthesize circuit, branch and order defect-free RRSS linkages to approximate N prescribed rigid-body positions. As illustrated in Fig. 2, the tibial position coordinates measured in stage 1 are used as rigid-body positions for stage 2. Given a series of tibial positions, the RRSS motion generation model will calculate the dimensions and driving link rotations of a circuit, branch and order defect-free RRSS linkage that approximates the prescribed tibial positions.

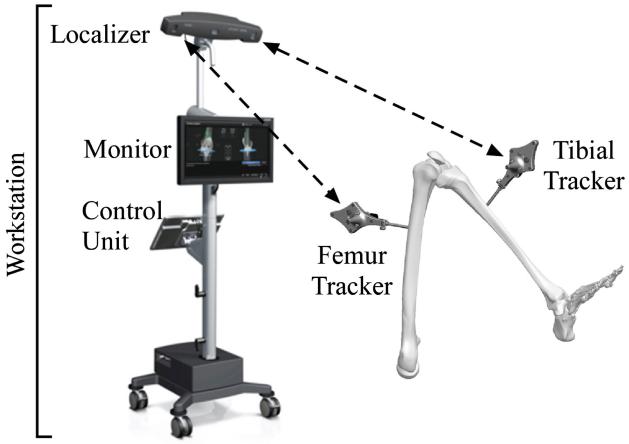

Fig. 3 Tibial-femoral position measurement system

Shen et al. [9] presented a model to generate the fixed and moving axodes for the RRSS linkage. As illustrated in Fig. 2, the RRSS linkage dimensions produced in stage 2 are used as input for stage 3. Given RRSS linkage dimensions and driving link rotations, the RRSS axode generation model will calculate the corresponding fixed and moving axodes. The coupler motion of the RRSS linkage (and subsequently the tibial positions achieved by this linkage) is replicated precisely by rolling the moving axode over the fixed axode [9].

Lastly, the fixed and moving axodes generated in stage 3 are incorporated into the geometry of a transfemoral prosthetic knee to replicate natural tibial motion.

3 Example

A series of tibial positions was measured using the approach in Sect. 2. Table 1 includes the spatial Cartesian coordinates measured for five tibial positions over approximately 37.5° of knee flexion (Fig. 4). This flexion range is adequate to describe the normal range for a standard gait cycle [2].

Table 1 Measured tibial position coordinates

Pos.	p (mm)	q (mm)	r (mm)
1	40.254, 2.718, −146.972	43.729, 2.845, −178.452	22.770, −11.562, −186.178
2	36.416, −6.936, −148.370	39.560, −9.379, −179.790	19.747, −26.032, −185.843
3	30.931, −34.024, −148.506	33.353, −42.460, −178.936	14.963, −61.578, −180.639
4	25.900, −80.564, −135.789	27.553, −97.742, −162.345	9.340, −116.529, −157.674
5	22.384, −117.358, −114.054	23.454, −140.564, −135.580	4.615, −157.026, −126.60

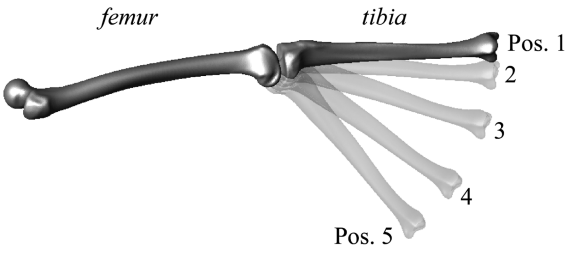

Fig. 4 Tibial displacement range

Table 2 Initial and calculated RRSS linkage dimensions and link rotation values

Variable	Initial values	Calculated values
a_0	−5, −30, −9	−8.277, −30.438, −9.119
a_1	−5, −15, 5.5	−2.525, −15.192, 4.150
ua_0	1, 0, 0	0.962, −0.194, −0.194
ua_1	1, 0, 0	0.962, −0.194, −0.194
b_0	−5, −2.8, −6.3	−5.447, −2.581, −5.130
b_1	−5, −22, 14.5	−3.407, −18.896, 14.761
θ_2–θ_5	10°…10°	0.723°, 3.027°, 8.609°, 15.387°
α_2–α_5	5°…5°	−5.062°, −18.387°, −42.512°, −65.086°

Table 3 Tibial position coordinates achieved by the synthesized RRSS linkage

Pos.	p (mm)	q (mm)	r (mm)
1	40.254, 2.718, −146.972	43.729, 2.845, −178.452	22.770, −11.562, −186.178
2	37.841, −7.915, −148.309	40.869, −10.034, −179.764	20.024, −25.261, −186.103
3	32.360, −35.434, −147.983	34.412, −43.217, −178.614	14.001, −60.045, −181.209
4	25.650, −81.213, −135.511	26.658, −97.927, −162.393	7.394, −115.776, −158.289
5	22.806, −116.926, −113.938	23.582, −140.062, −135.552	5.629, −157.064, −125.80

Next, the measured tibial position coordinates were used to synthesize an RRSS linkage to approximate these coordinates. Table 2 includes the initial and calculated values for the RRSS linkage using the RRSS motion generation model [8]. Table 3 includes the actual tibial position coordinates achieved by the synthesized RRSS linkage (Fig. 5).

Following RRSS motion generation is RRSS axode generation. Figure 5 also includes the fixed and moving axode sections generated using the RRSS axode generation model [9]. The tibial positions in Table 3 are perfectly replicated by rolling the moving axode section over the fixed axode section.

Lastly, the axodes are incorporated in prosthetic knee geometry. In Figs. 5 and 6, the axodes are expressed as noncircular gears (to eliminate slip during knee flexion and extension). Figure 6 also includes the Table 3 tibial positions achieved by the transfemoral prosthetic knee.

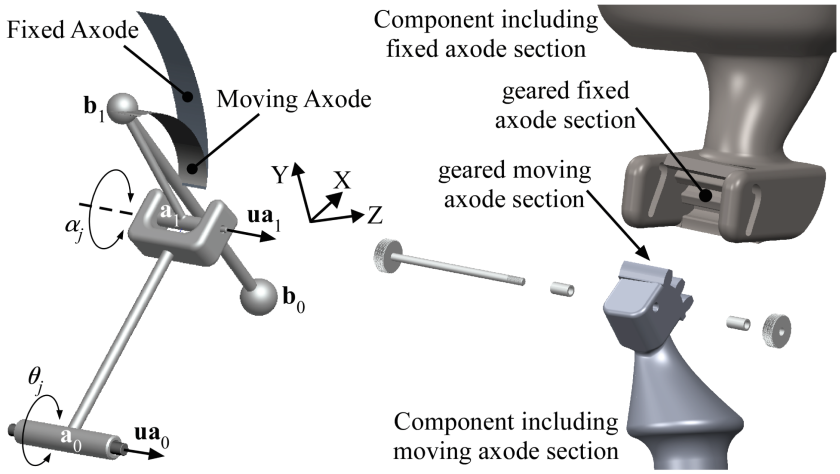

Fig. 5 Synthesized RRSS linkage with fixed and moving axode sections (*left*) and exploded view of transfemoral prosthetic knee (patent pending) with axode sections as gearing (*right*)

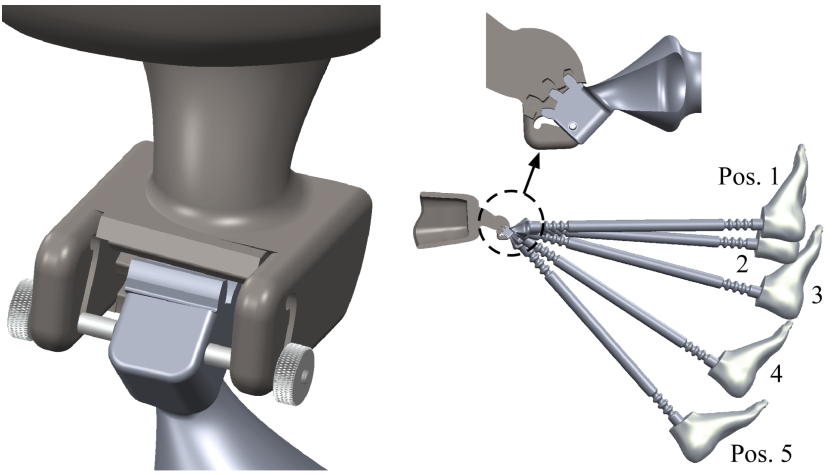

Fig. 6 Assembly view of transfemoral prosthetic knee (patent pending) (*left*) and achieved tibial positions in Table 3 (*right*)

4 Conclusions

Here, the design procedure for a prosthetic knee to achieve natural tibial motion is presented. Given a group of tibial positions, a defect-free RRSS linkage is first synthesized to approximate these positions. The fixed and moving axodes of the synthesized motion generator are calculated next. Lastly, these axodes are incorporated as gearing into a prosthetic knee design.

References

1. Frankel, V.H., Burstein, A.H., Brooks, D.B.: Biomechanics of internal derangement of the knee. J. Bone J. Surg. **53-A**(5), 945–977 (1971)
2. Benoit, D.L., Ramsey, D.K., Lamontagne, M., Xu, L., Wretenberg, P., Renström, P.: In vivo knee kinematics during gait reveals new rotation profiles and smaller translations. Clin. Orthop. Relat. Res. **454**(1), 81–88 (2007)
3. Dennis, D.A., Mahfouz, M.R., Komistek, R.D., Hoff, W.: In vivo determination of normal and anterior cruciate ligament-deficient knee kinematics. J. Biomech. **38**(2), 241–253 (2005)
4. Blankevoort, L., Huiskes, R., De Lange, A.: Helical axes of passive knee joint motions. J. Biomech. **23**(12), 1219–1229 (1990)
5. Hart, R.A., Mote, C.D., Skinner, H.B.: A finite helical axis as a landmark for kinematic reference of the knee. J. Biomech. Eng. **113**(2), 215–222 (1991)
6. Sheehan, F.T.: The finite helical axes of the knee joint (a non-invasive in vivo study using fast-PC MRI). J. Biomech. **40**(5), 1038–1047 (2007)
7. Van Den Bogert, A.J., Reinschmidt, C., Lundberg, A.: Helical axes of skeletal knee joint motion during running. J. Biomech. **41**(8), 1632–1638 (2008)
8. Russell, K., Shen, Q.: Expanded spatial four-link motion and path generation with order and branch defect elimination. Inverse Prob. Sci. Eng. **19**(2), 251–265 (2011)
9. Shen, Q., Russell, K., Lee, W., Sodhi, R.S.: On cam system design to replicate spatial four-bar mechanism coupler motion. Inverse Prob. Sci. Eng. **19**(2), 251–265 (2011)